analytical chemistry

Article

pubs.acs.org/ac

# Determination of Iron Content and Dispersity of Intact Ferritin by Superconducting Tunnel Junction Cryodetection Mass Spectrometry

Logan D. Plath, Abdil Ozdemir,[†] Alexander A. Aksenov,[‡] and Mark E. Bier*

Center for Molecular Analysis, Department of Chemistry, Carnegie Mellon University, 4400 Fifth Avenue, Pittsburgh, Pennsylvania 15213, United States

Supporting Information

**ABSTRACT:** Ferritin is a common iron storage protein complex found in both eukaryotic and prokaryotic organisms. Although horse spleen holoferritin (HS-HoloFt) has been widely studied, this is the first report of mass spectrometry (MS) analysis of the intact form, likely because of its high molecular weight ~850 kDa and broad iron-core mass distribution. The 24-subunit ferritin heteropolymer protein shell consists of light (L) and heavy (H) subunits and a ferrihydrite-like iron core. The H/L heterogeneity ratio of the horse spleen apoferritin (HS-ApoFt) shell was found to be ~1:10 by liquid chromatography−electrospray ionization mass spectrometry. Superconducting tunneling junction (STJ) cryodetection matrix-assisted laser desorption ionization time-of-flight MS was utilized to determine the masses of intact HS-ApoFt, HS-HoloFt, and the HS-HoloFt dimer to be ~505 kDa, ~835 kDa, and ~1.63 MDa, respectively. The structural integrity of HS-HoloFt and the proposed mineral adducts found for both purified L and H subunits suggest a robust biomacromolecular complex that is internally stabilized by the iron-based core. However, cross-linking experiments of HS-HoloFt with glutaraldehyde, unexpectedly, showed the complete release of the iron-based core in a one-step process revealing a cross-linked HS-ApoFt with a narrow fwhm peak width of 31.4 kTh compared to 295 kTh for HS-HoloFt. The MS analysis of HS-HoloFt revealed a semiquantitative description of the iron content and core dispersity of 3400 ± 1600 ($2\sigma$) iron atoms. Commercially prepared HS-ApoFt was estimated to still contain an average of 240 iron atoms. These iron abundance and dispersity results suggest the use of STJ cryodetection MS for the clinical analysis of iron deficient/overload diseases.

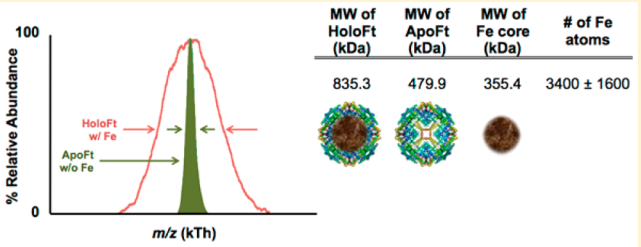


Ferritins encompass a large group of biomacromolecular complexes whose primary role involves the storage of iron in a nontoxic form within the body of the host. They are the only biomolecular complexes that provide an *in vivo* phase transition of iron between the solution and solid phase.[1] When free within the body, Fe(II) can react with oxygen and hydrogen peroxide to cause damaging free radicals through the Fenton reactions. Free radicals damage genetic material inside a cell as a result of oxidative stress.[2] To reduce the bioavailability of Fe(II) within the body, iron is withdrawn by holoferritin (HoloFt), oxidized, and stored as Fe(III). Upon biochemical signaling, Fe(III) is reduced and released from the ferritin cavity for use intracellularly. These processes have been studied extensively and these as well as the structure−function relationships in ferritins have been reviewed elsewhere.[1,3−19]

The general structure of ferritins, as a group, has been reported.[3,5,20] HoloFt is comprised of an approximately spherical protein shell made up of 24 nonidentical subunits and a mineralized iron-based core.[12] Without the iron-based core, ferritin is referred to as apoferritin (ApoFt). While protein subunits are nonidentical, two dominant subunits, H and L comprise the ApoFt shell in mammalian cells.[6] H refers to the heavier subunit with a mass of ~21 kDa and the L subunit is the lighter subunit of ~20 kDa. Although structurally similar, ferroxidase catalytic activity only takes place on the H subunit,[7] while L subunits have been proposed to provide nucleation sites for the mineralized iron core.[15] The H/L ratios vary from species to species and tissue to tissue. Tissues where ferroxidase activity is greatly needed have evolved to produce predominately H-rich ApoFt. Sequence homology of the active residues are highly conserved between species, and H and L subunits have tertiary structures consisting of four $\alpha$-helices, rendering an overall spherical ApoFt protein complex.[6] When fully assembled, the ApoFt shell has a theoretical mass of approximately 480 kDa. Together, ApoFt and the mineralized iron core has been reported to make up a bioinorganic protein complex with a mass as high as ~1 MDa at the maximum iron content.[7]

The iron core consists of an Fe(III) oxide complex that resembles the mineral ferrihydrite ($5Fe_2O_3 \cdot 9H_2O$).[21−23] The exact composition of the core is still not well understood, but X-ray and electron diffraction measurements performed by Towe and Bradley[21] corresponded to a chemical formula of $Fe_5HO_8 \cdot 4H_2O$ occupying a hexagonal unit cell with dimensions $a_0$ = 0.508 nm and $c_0$ = 0.940 nm. The ferrihydrite-like iron

**Received:** June 9, 2015
**Accepted:** August 12, 2015
**Published:** August 12, 2015





DOI: 10.1021/acs.analchem.5b02180
*Anal. Chem.* 2015, 87, 8985−8993

core has also been shown to contain various amounts of inorganic phosphate assumed to be adsorbed to the crystallite surfaces. The amount of phosphate adsorbed is dependent on nanoparticle size; however, the average phosphorus/iron ratio has been reported as ∼1:10 in horse spleen holoferritin (HS-HoloFt).[22,24,25] Descriptions of the HS-HoloFt quaternary structure were determined by Harrison[26] and Fischbach and Anderegg[27] using X-ray scattering techniques. They elucidated the size and dimensions of the protein complex describing the ApoFt shell with a 12.2 nm outer diameter and 7.4 nm central cavity.

It is not clear what laboratory first made the measurement of the number of iron atoms and the variability of this amount in ferritin. There has been some variability in these values over the years due to the chemical formula used, the quality of the core diameter measurement (e.g., X-ray resolution), and how the calculation was done. However, since at least 1977 through the present day,[28] numerous reports have stated without firm reference that HS-HoloFt can encapsulate up to a maximum of 4 500 iron atoms, as a ferric oxyhydroxide-like core within a 7.0−8.0 nm diameter protein cavity.[7,24,29−31] Haggis had previously reported in 1965 that a well-filled core could contain 5 000 iron atoms based on a core of FeOOH and a core diameter of 6.9−7.4 nm.[32] Fischbach and Anderegg, also in 1965, determined that an average of 4 300 iron atoms are contained in a "fully-filled" 418 kDa core with a diameter of 7.4 nm from sedimentation and small-angle X-ray scattering of HS-ApoFt and HS-HoloFt.[27,32] Salgado et al. developed a mathematical model to determine that a Fe/Ft ratio of 1 000:1 is optimal for iron buffering by horse spleen holoferritin (HS-HoloFt) in cultured cells, which is significantly lower than the typical average empirical ratios.[33] Other reports have stated that ferritins isolated from horse spleen have between 2 000 and 3 000 iron atoms per protein complex.[7,31] The wide range in the amount of calculated iron in the core is understandable given the broad range of iron core diameters, from 5.4 to 9.0 nm, that have been reported over the years.[34−36]

Reports have been made related to the stability of the HoloFt/ApoFt structure particularly as it relates to pH.[31] At neutral pH, ApoFt is observed to be highly stable even upon heating to 80 °C and in a 6 M guanidine environment.[1] A more recent report by Kim et al. has further explored the effects of pH on the ApoFt shell. They showed that ApoFt was stable between pH 3.40−10.00. The study also investigated the reassembly of the ApoFt when restoring neutral pH after first being subjected to disassociation and denaturation in low pH conditions. The degree of reassembly of ApoFt was further diminished when starting from lower pH solutions.[37]

Although there are many publications about ferritin, few investigators have used mass spectrometry (MS). Kaltashov and Mohimen utilized electrospray ionization (ESI)-MS to investigate surface charge phenomenon of human ApoFt and other proteins.[38] In 2006, de Val et al. measured the mass of horse ApoFt, made recombinately consisting entirely of the L subunit, to be 491.5 kDa, also by ESI-MS.[39] Other researchers have investigated modifications made to ApoFt/HoloFt *in vitro*.[40−42] Hoppler et al. have developed a quantitative method for measuring ferritin-bound iron in plant species utilizing isotope dilution MS.[40] Other groups have studied characteristics of the ferritin subunits using mass spectrometric proteomic techniques.[41−43] The lack of MS publications on intact ferritin is likely due to the fact that traditional MS techniques for HoloFt could not be utilized because of the high molecular weight and broad size distribution of the assembly. Here we present heavy ion mass spectrometry (HIMS) work above 100 kTh utilizing matrix-assisted laser desorption ionization (MALDI) time-of-flight (TOF) MS which incorporates a superconducting tunnel junction (STJ) cryodetector. STJ cryodetection is unique in that detection is mass independent and only requires a relatively low kinetic energy of the impinging ion for signal production.[44] A technical description and review of STJs may be found elsewhere.[45−47] Use of STJ detection at 1 MTh and higher have been reported for IgM (∼1 MDa)[48] and polystyrene (∼2 MDa)[49] highlighting the signal response observed even at these high $m/z$ values. Most remarkable are the STJ MS results for the capsids of bacteriophage HK97 which weigh 13 MDa and 17.7 MDa where, for the first time, individual charge states were separated and mass-analyzed by MS at this high mass.[50,51] Signal responses from a more typical ionizing detector, such as a microchannel plate (MCP) detector, coupled to a typical MALDI-TOF instrument would not achieve the S/N level required to be useful for most analyses at these high $m/z$.

Here we report the analysis of HoloFt and ApoFt isolated from horse spleen using MALDI-TOF-STJ MS and the H and L ferritin subunit monomers by liquid chromatography (LC) ESI-MS. The unique high mass detection made possible by STJ cryodetection allowed us to investigate the intact mass of HS-HoloFt and horse spleen apoferritin (HS-ApoFt) directly and to further understand some of the biomacromolecular characteristics that make ferritin distinguishable from other noncovalent protein complexes, namely, its stability and the amount and dispersity of iron loading.

## EXPERIMENTAL SECTION

A detailed description of experimental methods can be found in the Supporting Information. In brief, the protein subunit composition was investigated by reverse phase LC-ESI-MS. HS-HoloFt and HS-ApoFt samples were analyzed intact using a Macromizer MALDI-TOF mass spectrometer with a 16-channel STJ detector (Comet AG, Flamatt, Switzerland).[48] Chemical cross-linking of both HS-ApoFt and HS-HoloFt was performed by the addition of the homobifunctional cross-linker, glutaraldehyde. The reaction was monitored over time by MALDI-TOF-STJ MS.

## RESULTS AND DISCUSSION

**Ferritin Structure, Composition, and Subunit Analysis.** The structure of HS-HoloFt has been studied extensively.[20,37,52−59] The heteropolymer of HS-ApoFt has been reported to contain between 7 and 15% of the H-subunit.[60,61] The analysis of HS-ApoFt by reverse phase LC showed that the L-subunit is ∼10× greater in abundance than the H-subunit (see the Supporting Information Figure S1), which suggests a H/L ratio where H is 3, 2, or 1. Previous studies have elucidated the amino acid sequence of the L-subunit of HS-ApoFt and have proposed that the N-terminus is acetylated.[62] In the present study, the experimental molecular weight of HS-ApoFt was derived by determining the weights of the L and H subunits independently and by direct mass measurement of the intact complex. The ESI mass spectra for the L and H subunits are shown in Figure 1 with the deconvolved molecular weight (MW) plots shown as insets.

As shown in the inset in Figure 1a, upon deconvolution of a typical ESI mass spectrum for HS-ApoFt light chain, several


DOI: 10.1021/acs.analchem.5b02180
*Anal. Chem.* 2015, 87, 8985−8993

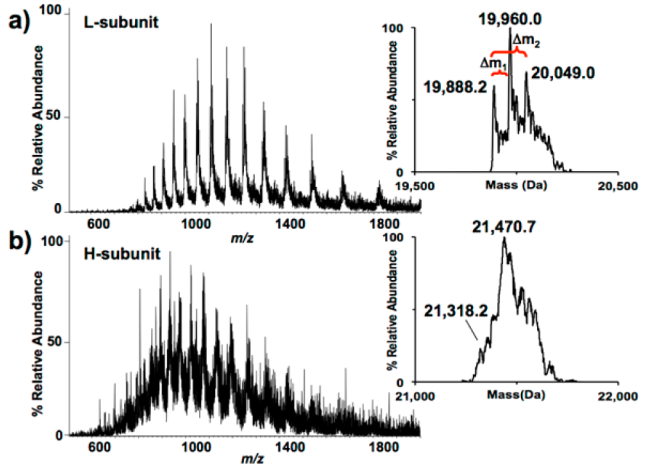


**Figure 1.** Electrospray ionization mass spectra of (a) HS-ApoFt, L-subunit (theoretical $MW_{avg}$ = 19 888.43 Da, experimental $MW_{avg}$ = 19 887.9 ± 2.8 Da) and of (b) HS-ApoFt, H-subunit (theoretical $MW_{avg}$ = 21 179.63 Da, experimental $MW_{avg}$ = 21 328.8 ± 18.0 Da) after reverse phase LC. The inset deconvoluted spectra from L and H subunits of HS-ApoFt show distinct peaks that may be attributed to modifications of the proteins from mineralization of the core or the presence of impurities. For example, the HS-ApoFt L monomer protein shows an adduct $\Delta m_1$ which is 71.8 Da higher in mass than the unmodified monomer molecular weight. This increase may correspond to a reduced iron oxide adduct, FeO (MW = 71.84 Da) or FeOH (theoretical MW = 72.85 Da), and the $\Delta m_2$ of 160.8 Da may correspond to $Fe_2HO_3$ (MW = 160.7 Da) and/or $Fe_2O_3$ at a theoretical MW of 159.7 Da as a result of incomplete demineralization.

spectral features were observed. Assigning the lowest mass peak in the deconvolved spectra as the acetylated protein, the average measured molecular weight ($MW_{avg}$) of the L-subunit was 19 887.9 ± 2.8 Da, which corresponded to the theoretical molecular weight of the acetylated protein from the sequence, 19 888.43 Da (UniProtKB ID: P02791). The second and most abundant mass peak of the inset spectra shown in Figure 1a at 19 960.0 Da corresponded to an increased $\Delta m_1$ of 71.8 Da. Given the chemical nature of the iron-based core, this peak was assigned to an iron oxide adduct (FeO, theoretical MW = 71.84 Da) or FeOH (theoretical MW = 72.85 Da), that remained bound to the protein after reduction and demineralization procedures by the manufacturer. The third major peak, observed at 20 049.0 Da, corresponded to an increase in a $\Delta m_2$ of 160.8 Da from the unmodified light chain and 89.0 Da from the light chain with the proposed FeO adduct. Again, given the nature of the iron-based core, we have assigned, although tentatively, this higher mass to the addition of $Fe_2O_3$ or $Fe_2HO_3$ at theoretical MWs of 159.7 and 160.7 Da, respectively.

While the gene for HS-ApoFt heavy chain has been determined,[63] direct measurement of the exact molecular weight by modern proteomic techniques have yet to be shown. Provided the methionine of the start codon was absent and the resulting N-terminus was acetylated, similarly to the L-subunit, the HS-ApoFt H-subunit would have a theoretical MW of 21 179.63 Da (UniProtKB ID: Q8MIP0). The deconvolution of the heavy chain ESI mass spectrum is shown in the inset of Figure 1b with a broad distribution of mass centered around 21 470 Da with a signal-to-noise ~10× less than that found for the L-chain. The presumed unmodified H-subunit, as measured using the lowest $m/z$ peak in the deconvoluted spectrum of the significantly lower signal ESI mass spectrum shown in Figure 1b, has a $MW_{avg}$ of 21 328.8 ± 18.0 Da. The $\Delta m$ difference of 149.2 Da from the expected theoretical molecular weight may be attributed to adducts of iron-based core species remaining within the biomacromolecular complex as found for the L-subunit, but the signal was not resolved well enough to make assignments. While distinguishable spectral features are absent from the H-subunit deconvolution, unlike for the L-subunit, both of these broad distributions, for both H and L, may be attributed to multiple overlapping peaks corresponding presumably to mineral adducts of iron oxide species that have been retained on the subunit. Given the reverse phase LC methods employed, it is unlikely that common electrospray adducts such as sodium or potassium cations are the cause for the broad mass distributions observed for both subunit species. The observation of broad adduct peaks and mass distributions of ferritin subunits after chromatography suggest a high affinity for pieces of the iron-based core to the individual protein subunits.

From the above $MW_{avg}$ determined for the L and H protein subunits and by assuming a H/L of 2:22, an expected molecular weight of the HS-ApoFt complex was calculated to be 480.2 ± 0.03 kDa. The theoretical $MW_{avg}$ of unmodified HS-ApoFt is 479.9 kDa. These molecular weights of the apoprotein isoforms are in good agreement, but when considering the observation of the abundant adducts found on both HS-ApoFt subunits as discussed above, an increase in mass and a broad peak would be expected in the MALDI-TOF-STJ MS analyses of the intact complex.

**MALDI-TOF-STJ MS of the Apoferritin and Ferritin Complexes.** On the basis of the existing body of work described in the literature and the separation of subunits experimentally (Supporting Information Figure S1), the data supports that the assembled HS-ApoFt complex should contain 1 to 3 H-subunits. On the basis of the theoretical molecular weight of the H-subunit, a HS-ApoFt complex with 1, 2, or 3 H-subunits would have an average theoretical MW of 478.6 kDa, 479.9 kDa, and 481.2 kDa, respectively.[60,64] Using a MALDI-TOF mass spectrometer equipped with a STJ cryodetector, we were able to observe the singly and doubly charged ions of HS-ApoFt and the HS-ApoFt dimer, as shown in Figure 2. The base peak at 504.8 kTh is the broad +1 charge state of HS-ApoFt followed at ~25% relative abundance by the +2 charge state at 256.3 kTh. The singly charged HS-ApoFt dimer was found at 1 018.2 kTh at an expected reduced abundance. All ions are significantly above the unmodified theoretical MW, which could be attributed, at least in part, to insufficient mineral removal by the commercial supplier and the possibility of cargo loading of the cavity with matrix or solvent. The rise of the baseline at less than 200 kTh has been assigned to matrix clusters of sinapinic acid, commonly observed in MALDI analysis.

As can be seen in Figure 2, unlike conventional MS using an ionizing detector, the STJ provides a third dimension of information. In addition to signal intensity and $m/z$, the STJ cryodetector allows for discrimination of the relative ion impact energy (for discussion of three-dimensional STJ MS data and scatterplot images refer to the Supporting Information). This energy information, when resolved, allows for the visualization and determination of charge states such as for the doubly charged ion at 256.3 kTh and can separate overlapping $m/z$ values as shown for singly charged HS-ApoFt at 504.8 kTh from the lower abundant doubly charged dimer at 514.6 kTh.


DOI: 10.1021/acs.analchem.5b02180
Anal. Chem. 2015, 87, 8985−8993

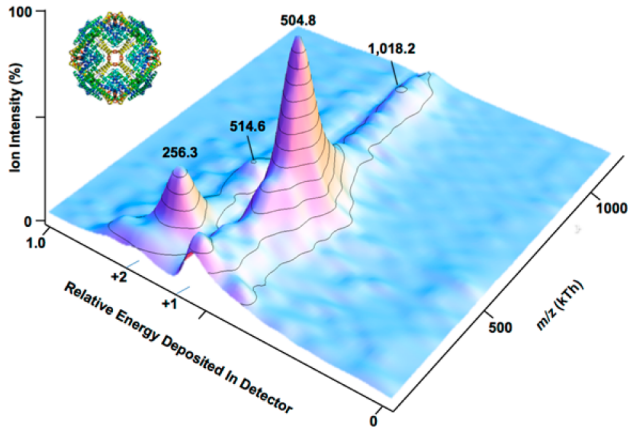


**Figure 2.** MALDI-TOF-STJ 3D-mass spectrum of HS-ApoFt. The ions shown at $m/z$ 504.8, 256.3, 1018.2, and 514.6 consist of $[M + X]^+$, $[M + 2X]^{+2}$, $[2M + X]^+$, and $[2M + 2X]^{+2}$, respectively, where X is a cation such as $H^+$ or $Na^+$. Note that the broad peak widths and molecular weight ~25 kDa greater than the theoretical mass suggests that the protein complex is not entirely free from bound material. (Inset shows crystal structure of PDB 1IER).

The higher $m/z$ assignment for the doubly charged dimer ion is likely due to an increased mass error as a result of the lower ion abundance statistics. In any regard, the determination of charge state by detector response is a valuable feature not available on conventional mass spectrometers.

To further understand the reasons behind peak broadening for the HS-ApoFt complex, peak shapes from multimers of monoclonal IgG1 antibody were used for a peak width comparison. Figure 3 shows the overlaid normalized 2D-mass

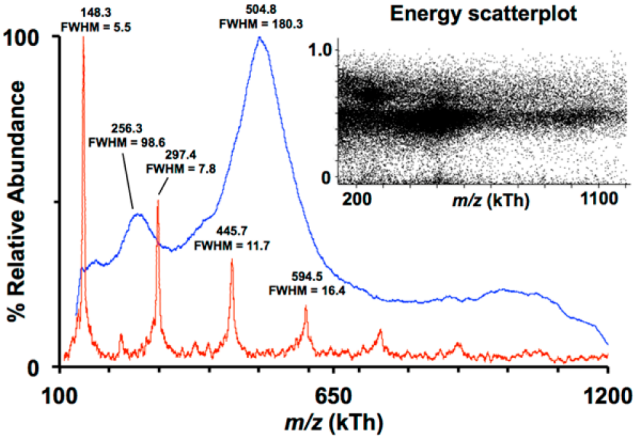


**Figure 3.** MALDI-TOF-STJ mass spectrum of HS-ApoFt (blue) in comparison with monoclonal IgG1 antibody (red). Both spectra were acquired on the same day under identical preparations and instrumental parameters. The broadened spectral peaks for HS-ApoFt suggest that it may still strongly bind mineral adducts and that common commercial preparation techniques did not produce "true" ApoFt completely free of the iron. Inset graph shows a scatterplot of HS-ApoFt generated during the MALDI-TOF-STJ MS analysis.

spectra of assembled HS-ApoFt (blue trace) and that of monoclonal IgG1 (red trace). The trimer $[3M + H]^+$ (445.5 kTh) and tetramer $[4M + H]^+$ (594.0 kTh) of IgG1 $m/z$ bracket the singly charged ion of HS-ApoFt. At a fwhm of 180.3 kTh, the HS-ApoFt peak width is ~11× larger than the IgG1 tetramer $[4M + H]^+$ at a fwhm of 16.4 kTh. The broad mass peaks shown in the mass spectra of Figures 2 and 3, for what should be otherwise a monodispersed HS-ApoFt complex, are likely due to a number of contributing factors including isotope distribution, various amounts of cationization (e.g., $Na^+$, $K^+$), fragmentation, adduction of matrix and buffer molecules, adduction of free L and H-subunits, and perhaps significant adduction of residual bound mineral of the ferrihydrite-like core to the iron-free protein of 480 kDa. As mentioned already, the retention of some mineral adducts likely remain after iron reduction and demineralization. In addition, since HS-ApoFt is a closed shell "empty" complex, small molecules such as matrix and solvent may have entered the shell prior to or during the MALDI preparation steps to "load" the cavity and these molecules may not be fully released before mass analysis due to steric hindrance of the protein cage. Since the complex was unexpectedly high in mass with a broad peak width, we also purchased a second sample of HS-ApoFt from a different manufacturer, but the mass spectrum showed an even higher and broader mass peak with reduced signal-to-noise.

To further investigate the structural stability of ferritin when loaded with its ferrihydrite-like core and the capabilities of STJ cryodetectors for applications in HIMS, the HS-HoloFt complex was analyzed. Figure 4 shows the 3D-histogram

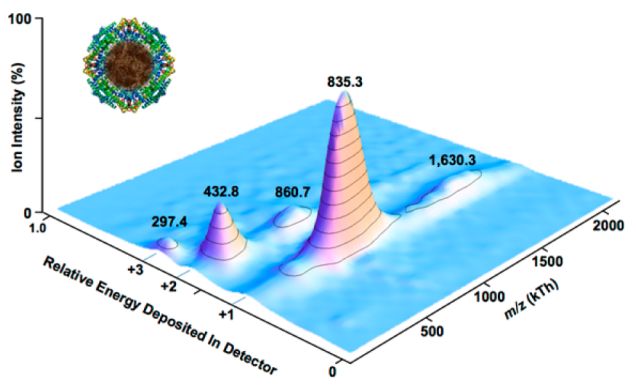


**Figure 4.** MALDI-TOF-STJ 3D-mass spectrum of HS-HoloFt. The peaks are assigned to $[M + X]^+$, $[M + 2X]^{+2}$, $[M + 3X]^{+3}$, $[2M + X]^+$, and $[2M + 2X]^{+2}$ ions for 835.3, 432.8, 297.4, 1630.3, and 860.7 kTh, respectively, where X is a cation. Note the broad dispersity of the peaks, which is primarily attributed to the variation in size of the iron-based core (Inset shows the crystal structure with illustrative iron core based on PDB 1IER).

mass spectrum of the HS-HoloFt complex with five spectral $m/z$ peaks and three energy regions centered and identified as the 1+, 2+, and 3+ charge states. Similarly to the HS-ApoFt data shown in Figure 2, spectral peaks with overlapping $m/z$ such as $[M + X]^+$ at 835.3 kTh and $[2M + 2X]^{2+}$ at 860.7 kTh, where X represents a cation, were energy resolved. This is the first mass spectrum known for intact HS-HoloFt and it highlights the high-mass sensitivity of the STJ cryodetectors.

As shown in Figure 4, the peak width of the 1+ charge state of HS-HoloFt is broad. As has been suggested by others,[34,35] HS-HoloFt contains a distribution of the amount of iron atoms in a form similar to ferrihydrite. In addition, there are contributions to the peak width due to the natural isotope distribution of atoms in the monodispersed protein complex and the iron core. Assuming that there are no other significant contributions to the peak width between HS-HoloFt and HS-ApoFt, the peak width in the $m/z$ dimension can be used to describe the dispersity of the iron core. That is, when HS-


DOI: 10.1021/acs.analchem.5b02180
Anal. Chem. 2015, 87, 8985−8993

Table 1. Quantification and Dispersity of Iron in Horse Spleen Holoferritin and Apoferritin

| | $m/z$ of singly charged ion (kTh) | $\Delta m$ from theoretical MW[a] (kDa) | peak width at fwhm (kTh) | no. of Fe atoms | avg Fe core diameter (nm) |
|---|---|---|---|---|---|
| HS-HoloFt | 835.3 | 355.4 | 294.9 | 3400 ± 1600[b] | 6.5 |
| HS-ApoFt[c] | 504.8 | 24.9 | 180.3 | 240 | 2.7 |
| HS-ApoFt-CL[d] | 524.5 | 44.6 | 61.6 | | |
| HS-ApoFt-CL product from HS-HoloFt (3 h) | 530.6 | 50.7 | 31.4 | | |
| maximum HS-HoloFt[e] | | | | 5050 | 7.4 |
| avg HS-HoloFt[f] | | | | 2400 | 5.8 |

[a]Theoretical MW HS-ApoFt = 479.9 kDa (H/L = 2:22). $\Delta m$ refers to a positive mass change. [b]The ± 1600 represents the maximum variability at $2\sigma$ for the number of iron atoms contained in HS-HoloFt. [c]The iron dispersity was not generated for HS-ApoFt due to partial fragmentation and there may be a mass contribution from trapped molecules inside the protein cage. [d]CL = glutaraldehyde cross-linker. [e]Based on uniform packing of the hydrated ferric oxide ($Fe_5HO_8{\cdot}4H_2O$; defect-free) in a spherical cavity (diameter = 7.4 nm) neglecting any contribution from phosphate.[21,27] [f]Determined by X-ray scattering and electron microscopy techniques.[65]

HoloFt is compared to pure HS-ApoFt, the difference in mass and peak width should theoretically be attributed entirely to the core.

The dispersity of HS-ApoFt and HS-HoloFt can be compared by measurement of the peak widths at full width at half-maximum (fwhm). Table 1 provides a comparison of the peak widths observed between commercially available samples of HS-ApoFt (see Figure 2) and HS-HoloFt (see Figure 4). These peak widths of 180.3 and 294.9 kTh, respectively, show that the HS-HoloFt complex is significantly more disperse than HS-ApoFt (see Supporting Information Figure S2) as expected; however, HS-ApoFt peak widths are also, unexpectedly, broad as previously discussed. The HS-ApoFt peak broadening may be partially attributed to the loss of stability as the iron core is reduced in size, allowing for increased fragmentation during the MALDI process. We hypothesize that the iron-based core adds significant structural stability via some form of internal bonding from the iron-based core to the protein shell. For ferritin, the protein−protein bonds are primarily noncovalent.[9,12] HS-ApoFt fragmentation was confirmed by chemically cross-linking the complex with glutaraldehyde, which showed an increased $MW_{avg}$ due to the addition of cross-linking reagents, but with a remarkably reduced peak width from 180.3 to 61.6 kTh fwhm (see Table 1 and Supporting Information Figure S3). Some evidence of fragmentation can also be seen in Figure 2, with tailing shown toward lower $m/z$ values.

**Iron Content in HS-ApoFt and HS-HoloFt.** Determining an accurate number of iron atoms inside the ferritin shell has been a long-standing problem. Past measurements used either sedimentation or X-ray methods, which had resolution errors as large as 10%. In the X-ray case, this error would propagate into the iron core volume calculation. Despite this error level, the value of 4 500 iron atoms[7,24,29−31] as the upper limit in HS-HoloFt has been used repeatedly throughout the literature without a definitive reference to the original work. In 1993, Massover questioned whether this value was 2× too high.[9] In the case described here, MS should allow for an improved mass accuracy measurement but, of course, any variance in the sample quality would remain the same.

Assuming that the iron core has a composition of $Fe_5HO_8{\cdot}4H_2O$ and contains a phosphate/iron ratio of 1:10 (i.e., $Fe_5HO_8{\cdot}4H_2O{\cdot}0.5PO_4$), one can semiquantitatively describe the iron content in ferritin directly from the MALDI-TOF-STJ MS data. Ideally, these values would be calculated by using the empirically determined masses and peak widths of HS-HoloFt and HS-ApoFt, however, since we were unable to determine the "true" mass and peak width of HS-ApoFt, we used the theoretical $MW_{avg}$ of HS-ApoFt (479.9 kDa) and assumed that the contributions to the peak width due to the protein were minimal based on the factors discussed earlier. Hence, the average number of iron atoms was determined by subtracting the theoretical $MW_{avg}$ of HS-ApoFt from the mass of HS-HoloFt and then calculating the iron content based on the chemical formula. Similarly, the maximum variability of iron atoms was determined by measuring the peak width of HS-HoloFt directly at the $\pm 2\sigma$ value (see the Supporting Information). As listed in Table 1, the iron content of HS-HoloFt was determined to be 3400 ± 1600 ($2\sigma$) iron atoms. Similarly, the increased mass of HS-ApoFt from the theoretical value may be attributed to retention of some iron core species as a result of incomplete demineralization. In the HS-ApoFt sample tested, 240 iron atoms were determined present. The dispersity of the iron core distribution in HS-ApoFt was not determined because the mass peak showed evidence of fragmentation compared to cross-linked HS-ApoFt (see Figures 2 and 3 and Figure S3).

The upper limit of the elemental iron capacity can also be approximated for HS-HoloFt based on a geometric analysis of a ferrihydrite-like lattice and the size of the protein cavity. The iron based core in HS-HoloFt has been proposed to have a formula $Fe_5HO_8{\cdot}4H_2O$.[21] Using the symmetry and lattice constants derived from X-ray and electron scattering studies, the volume of a single lattice is calculated to be 0.210 $nm^3$.[21] Neglecting any contribution from phosphate and assuming a single crystalline core with no defects filling a spherical cavity with a diameter of 7.4 nm, the maximum iron loading would be ∼5 050 iron atoms (see the Supporting Information). This upper limit estimation is reasonable when compared to the MS determined $2\sigma$ confidence level of iron loading of ∼5 000 iron atoms, which considered the contribution due to phosphate. The average MS determined value of 3 400 iron atoms shows that the mean ferritin iron core does not entirely fill the protein cavity to its maximum spatial capacity but is slightly higher than what would be expected for HS-HoloFt based on average core sizes of 5.8 nm (calculated iron content, 2 400 Fe atoms) reported from X-ray scattering and electron microscopy data.[65] Using a similar spatial calculation to determine iron capacity, average iron core size as observed by MALDI-TOF-STJ MS can be inferred to be approximately 6.5 nm (see Table 1). The determination of iron core size based on the MALDI-TOF-STJ MS data can also be extended to the MS analysis of HS-ApoFt, where the average iron core diameter retained by commercially prepared HS-ApoFt was calculated as 2.7 nm (240 Fe atoms). Again, it should be noted that the iron amount and dispersity


DOI: 10.1021/acs.analchem.5b02180
Anal. Chem. 2015, 87, 8985−8993

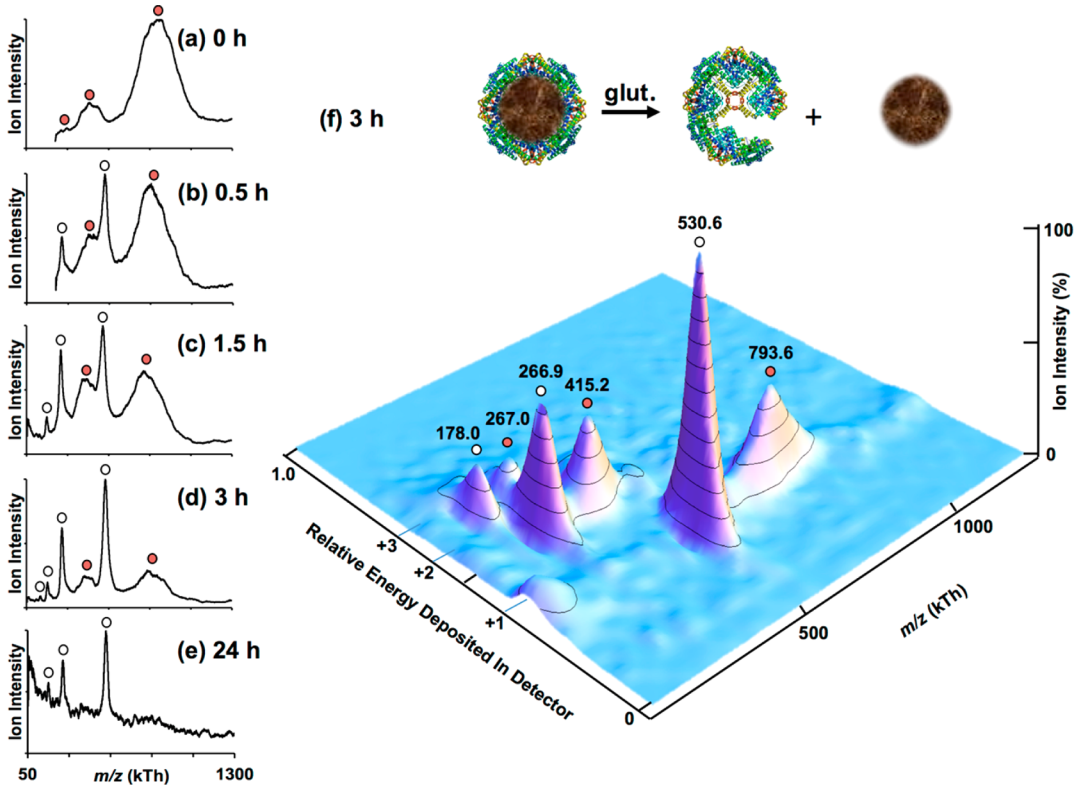


**Figure 5.** MALDI-TOF-STJ mass spectra of HS-HoloFt (red ●) and the formation of HS-ApoFt (○) over a 24 h reaction period of cross-linking with glutaraldehyde. Cross-linking (CL) was initiated by the addition of glutaraldehyde (1.25% w/v) in a bicarbonate buffer system (pH 9.6) and then a sample was collected after (a) 0, (b) 0.5, (c) 1.5, (d) 3, and (e) 24 h. The white circles represent the cross-linked HS-ApoFt peaks while the solid red circles represent HS-HoloFt and cross-linked HS-HoloFt peaks. Graph (a) shows HS-HoloFt at 0 h with no loss of the iron core while graph (e) shows little remaining HS-HoloFt and mostly cross-linked HS-ApoFt. The 3D-histogram mass spectrum of the cross-linked products after 3 h is shown in graph (f) illustrating the unexpected loss of the iron-core and the transition from dispersed HS-HoloFt-CL, due to the iron-based core, to a more monodispersed HS-ApoFt-CL. Glutaraldehyde is believed to disrupt the binding domain of the protein subunits, opening up the complex and ejecting the iron core in one step, yet it likely maintains some form of the HS-ApoFt assembly.

for HS-HoloFt and even more so for HS-ApoFt could be on the high side due to additional small molecule cargo (matrix or solvent) unable to exit the protein cage during the MALDI process. In any regard, it is reasonable to have a less than full capacity core since space between the inside of the protein cavity and the iron-core, and between the iron-core crystals themselves, would provide more surface area for efficient release or uptake of iron.

The advantages of determining the iron loading level in ferritin by this MALDI-TOF-STJ MS method may have a clinical application. For example, MS analysis uses tens of thousands of HS-HoloFt complexes in the measurement for good statistical analysis as compared to approximately 50−100 complexes as used in electron microscopy techniques. Additionally, the measurement is rapid since MS is done in the gas phase. Patients are often given a serum ferritin test to assess their level of anemia or iron deficiency; however, to the best of our knowledge, the distribution of iron in the human-HoloFt complex is not measured. An individual could have a high number of HoloFt complexes, but these complexes might be filled to a low or high iron abundance due to a genetic abnormality or disease. With MALDI-TOF-STJ MS we have shown that the iron dispersity could easily be measured, and perhaps such analysis could test for ferritin related diseases.

**Cross-Linking Ferritin with Glutaraldehyde.** While some secreted ferritins, most commonly found in insects, do exhibit intra- and intersubunit disulfide bonds, cytoplasmic mammalian ferritins, such as HS-HoloFt, do not.[3,6,7,12,66] As a result, the HS-HoloFt complex could dissociate during sample preparation due to the high concentration of organic solvent and matrix or during the MALDI process itself. Specifically, during the sample spot preparation, the protein is subjected to a phase transition from a highly organic liquid solution to a crystalline organic solid, neither of which is "native-like" in composition. Although organic solvents can cause dissociation, volatile solvents may also facilitate faster, homogeneous drying that may avoid extensive dissociation. Sample preparation solvent systems also often contain a small percentage of trifluoroacetic acid, formic acid, or acetic acid to assist in the protonation and separation of the protein. All of these non-native conditions would be expected to disturb both the tertiary and quaternary structure of a biomacromolecular complex even before the ion is formed in the gas phase in the MALDI source of the mass spectrometer. In addition, heating from the MALDI process can cause fragmentation; however, significant signal from metastable ion decomposition at lower energies than the 1+ charge state was not observed as shown the 3D-mass spectra in Figures 2, 4, and 5. To reduce the effects of these "non-native" conditions, cross-linking with glutaraldehyde was used to preserve the overall structural integrity of the HS-HoloFt complex. Glutaraldehyde reacts with any available primary amines, including itself, through self-polymerization reactions, and was used in molar excess to cross-link (CL) adjacent L or H subunits of the ferritin shell.


DOI: 10.1021/acs.analchem.5b02180
*Anal. Chem.* 2015, 87, 8985−8993

As shown in Figure 5, the addition of glutaraldehyde did not enhance the overall shell−core biomacromolecular complex stability but, unexpectedly, disturbed the HS-HoloFt complex in what appears to be at least a partial fracturing of the shell and release of the iron-core contrary to our original hypothesis.

By monitoring the cross-linking reaction with time, it was observed that after 30 min (Figure 5b), half of the HS-HoloFt-CL complexes have lost the iron-based core. As shown in Figure 5c, greater than half of the HS-HoloFt-CL complexes have lost the iron-based core at 1.5 h and by 3 h of reaction time, Figure 5d, only ∼20% of the HS-HoloFt complex remains. Although the spectrum in Figure 5e has a low signal level, possibly due to glutaraldehyde now blocking the basic amines groups from cationization, the nearly full conversion to what is expected to be some form of a cross-linked version of HS-ApoFt was observed after 24 h. There are three striking features of this data set: (i) the HS-HoloFt at $m/z$ 835 kTh, as shown in Figure 4, has presumably lost a ∼304 kDa mineralized iron-core resulting in a cross-linked "HS-ApoFt-CL" at $m/z$ 530.6 kTh as described above; (ii) the peak width of the newly formed HS-ApoFt-CL product, despite being cross-linked, was measured to be 31.4 kTh at fwhm, a value ∼17% the peak width of the commercially prepared HS-ApoFt shown in Figures 2 and 3; and (iii) although the molecular weight of the newly formed HS-ApoFt-CL is less than HS-HoloFt-CL, its average charge state is greater. The shift to a reduced peak width is due to the loss of the dispersed iron-based core leaving behind primarily the protein complex; however, it is noted that the energy spread increased due to metastable fragmentation over the HS-HoloFt-CL signal demonstrating a loss in stability of the HS-ApoFt-CL isoform although cross-linked (see Figure S4 in the Supporting Information). The shift to a higher charge state is likely due to the unhindered surface area on the inside surface of the HS-ApoFt-CL complex that can now accommodate more cations.[38] We hypothesize that upon addition of glutaraldehyde reacting with free amine groups of the HS-HoloFt complex, a change in tertiary structure of L or H or both subunits occurs. Since the 24-mer complex is noncovalently assembled, neglecting any protein-to-core bonds that likely exist given the adducts found from the LC−MS data, a change in tertiary structure may then induce a change in quaternary structure where the spherical complex opens up and releases the iron-core. MS analysis does not allow us to determine the final shape of the opened HS-ApoFt-CL shell after the core loss, but it would not be expected to reform the spherical shell shape given the above conditions and the explanation of disassembly via core ejection. It is likely that the structure and composition of the iron-core plays an important role in maintaining the quaternary structure of native HS-HoloFt and that the presence of glutaraldehyde may indeed perturb this association. Under basic conditions, the reactions of unsaturated oligomeric forms of aldehyde are likely. This leads to a wide array of possibilities of potential reaction mechanisms leading to the transformation of the HS-HoloFt moiety. Note that this conversion of HS-HoloFt to some form of HS-ApoFt-CL with glutaraldehyde addition does not occur by a steady reduction of the iron-based core, which would suggest some form of slow chemical dissolution of the iron-based core. A slower dissolution reaction would have shown a continuous shift to a lower mass and reduced peak width of the HS-HoloFt-CL starting material over time. Instead, the mass spectrum shows that the reaction occurs by a one-step process of opening the HS-HoloFt-CL shell followed by loss of nearly the entire iron-based core and hence an immediate mass shift from ∼800 kDa to the new product at ∼500 kDa. However, given this description above, there was no strong evidence for the iron-based core in the mass spectra. Calculating the number of iron atoms that might remain after iron-based core removal, as was shown in Table 1, is more elusive in this case since the HS-ApoFt-CL is now cross-linked with glutaraldehyde and it is not clear whether some of the L and H subunits may have been ejected with the core. In any regard, the mass of the HS-ApoFt-CL is greater by 26 kDa over the commercially prepared HS-ApoFt shown in Figure 2. At least in part, this mass increase may be attributed to the glutaraldehyde cross-linker addition since up to ∼224 amine moieties (2:22 H/L isoform) are available. The low dispersity of the formed HS-ApoFt-CL complex also suggests that the glutaraldehyde units do not substantially widen the peak. To the best of our knowledge, this interesting ejection of the iron-based core phenomena is a new observation.

## CONCLUSIONS

MALDI-TOF-STJ MS is a useful tool to study biologically relevant macromolecular protein complexes such as ferritin. Herein we have shown evidence for the mass measurement of the intact HS-HoloFt at 835 kDa and the HS-ApoFt complex at 504 kDa with no additional stabilization. Both LC-ESI-MS of the ferritin subunits and MALDI-TOF-STJ MS of the assembled complexes indicate that the HS-ApoFt complex has exceptional affinity for the iron based biomineral core and this core likely stabilizes the overall structure due to the internal bonding of the subunits. This report provides further evidence for the stability of the ferritin complex to extreme environmental stresses and provides a platform to expand the use of STJ cryodetection MS for the study of select fully intact complexes. STJ cryodetection allowed for the discrimination of energy levels between spectral peaks with the same $m/z$ value, showing that individual charge states can actually be a combination of multimeric ions, which would go undetermined using conventional MS instruments. A comparison of HS-ApoFt and HS-HoloFt mass and peak widths by MALDI-TOF-STJ MS can be used to investigate iron loading and the dispersity of the iron-core, which may be of practical relevance in research and in the diagnosis of ferritin related diseases.

## ASSOCIATED CONTENT

### Supporting Information

The Supporting Information is available free of charge on the ACS Publications website at DOI: 10.1021/acs.analchem.5b02180.

Detailed experimental methods, additional data and interpretation, and discussion of the calculations for determining iron content and core size (PDF)

## AUTHOR INFORMATION

### Corresponding Author

*Phone: (412) 268-3540. E-mail: mbier@andrew.cmu.edu.

### Present Addresses

†A.O.: Department of Chemistry, Sakarya University, Serdivan, Sakarya, 54187, TR

‡A.A.A.: Bioinstrumentation and BioMEMS Laboratory, Mechanical and Aerospace Engineering, University of California Davis, Davis, CA 95616, USA



DOI: 10.1021/acs.analchem.5b02180
Anal. Chem. 2015, 87, 8985−8993

### Notes

The authors declare no competing financial interest.

## ■ ACKNOWLEDGMENTS

We thank the late Prof. Robert Cotter for the donation of his Comet AG Macromizer instrument. We thank the NSF for funding under Grants DBI 0454980 and DBI 9729351. We thank David Sipe for helpful discussions and for his help with the demineralization of the ferritin and Rongchao Jin for useful discussion related to the "ferrihydrite-like" nanoparticle cores. We thank Gordon Rule for the initial supply of horse spleen ferritin and Fan Wang and Jonathan Feldman for their help in Mathematica programming. Finally we acknowledge the use of the Center for Molecular Analysis at Carnegie Mellon University.

## ■ REFERENCES

(1) Liu, X.; Theil, E. C. *Acc. Chem. Res.* **2005**, *38*, 167−175.
(2) Friedman, A.; Arosio, P.; Finazzi, D.; Koziorowski, D.; Galazka-Friedman, J. *Parkinsonism Relat. Disord.* **2011**, *17*, 423−430.
(3) Andrews, S. C.; Arosio, P.; Bottke, W.; Briat, J. F.; von Darl, M.; Harrison, P. M.; Laulhère, J. P.; Levi, S.; Lobreaux, S.; Yewdall, S. J. *J. Inorg. Biochem.* **1992**, *47*, 161−174.
(4) Granick, S. *Chem. Rev.* **1946**, *38*, 379−403.
(5) Haldar, S.; Bevers, L. E.; Tosha, T.; Theil, E. C. *J. Biol. Chem.* **2011**, *286*, 25620−25627.
(6) Harrison, P. M.; Lilley, T. H. In *Iron Carriers and Iron Proteins*; Loehr, T. M., Ed.; VCH Publishers, Inc.: New York, 1989; pp 123−238.
(7) Harrison, P.; Arosio, P. *Biochim. Biophys. Acta, Bioenerg.* **1996**, *1275*, 161−203.
(8) Harrison, P. M.; Andrews, S. C.; Artymiuk, P. J.; Ford, G. C.; Guest, J. R.; Hirzmann, J.; Lawson, D. M.; Livingstone, J. C.; Smith, J. M. A.; Treffry, A.; Yewdall, S. J. *Adv. Inorg. Chem.* **1991**, *36*, 449−486.
(9) Massover, W. H. *Micron* **1993**, *24*, 389−437.
(10) Rice, D. W.; Ford, G. C.; White, J. L.; Smith, J. M. A.; Harrison, P. M. *Adv. Inorg. Biochem.* **1983**, *5*, 39−50.
(11) Testa, U. In *Proteins of Iron Metabolism*; CRC Press LLC: Boca Raton, FL, 2002; pp 449−539.
(12) Theil, E. C. *Annu. Rev. Biochem.* **1987**, *56*, 289−315.
(13) Theil, E. C. *Adv. Inorg. Biochem.* **1983**, *5*, 1−38.
(14) Theil, E. C. *Inorg. Chem.* **2013**, *52*, 12223−12233.
(15) Theil, E. C.; Behera, R. K.; Tosha, T. *Coord. Chem. Rev.* **2013**, *257*, 579−586.
(16) Theil, E. C. *Curr. Opin. Chem. Biol.* **2011**, *15*, 304−311.
(17) Tosha, T.; Ng, H.-L.; Bhattasali, O.; Alber, T.; Theil, E. C. *J. Am. Chem. Soc.* **2010**, *132*, 14562−14569.
(18) Tosha, T.; Behera, R. K.; Ng, H.-L.; Bhattasali, O.; Alber, T.; Theil, E. C. *J. Biol. Chem.* **2012**, *287*, 13016−13025.
(19) Watt, R. K.; Frankel, R. B.; Watt, G. D. *Biochemistry* **1992**, *31*, 9673−9679.
(20) Granier, T.; Gallois, B.; Dautant, A.; Langlois d'Estaintot, B.; Précigoux, G. *Acta Crystallogr., Sect. D: Biol. Crystallogr.* **1997**, *53*, 580−587.
(21) Towe, K. M.; Bradley, W. F. *J. Colloid Interface Sci.* **1967**, *24*, 384−392.
(22) Chasteen, N. D.; Harrison, P. M. *J. Struct. Biol.* **1999**, *126*, 182−194.
(23) Jansen, E.; Kyek, A.; Schäfer, W.; Schwertmann, U. *Appl. Phys. A: Mater. Sci. Process.* **2002**, *74*, 1004−1006.
(24) Trefry, A.; Harrison, P. M. *Biochem. J.* **1978**, *171*, 313−320.
(25) Towe, K. M. *Origin, Evolution, and Modern Aspects of Biomineralization in Plants and Animals* **1989**, 265−272.
(26) Harrison, P. M. *J. Mol. Biol.* **1963**, *6*, 404−422.
(27) Fischbach, F. A.; Anderegg, J. W. *J. Mol. Biol.* **1965**, *14*, 458−473.
(28) Jutz, G.; van Rijn, P.; Santos Miranda, B.; Böker, A. *Chem. Rev.* **2015**, *115*, 1653−1701.
(29) Harrison, P. M. *Semin. Hematol.* **1977**, *14*, 55−70.
(30) Williams, J. M.; Danson, D. P.; Janot, C. *Phys. Med. Biol.* **1978**, *23*, 835−851.
(31) Webb, B.; Frame, J.; Zhao, Z.; Lee, M.; Watt, G. *Arch. Biochem. Biophys.* **1994**, *309*, 178−183.
(32) Haggis, G. H. *J. Mol. Biol.* **1965**, *14*, 598−602.
(33) Salgado, J. C.; Olivera-Nappa, A.; Gerdtzen, Z. P.; Tapia, V.; Theil, E. C.; Conca, C.; Nuñez, M. T. *BMC Syst. Biol.* **2010**, *4*, 147−162.
(34) Stuhrmann, H. B.; Haas, J.; Ibel, K.; Koch, M. H.; Crichton, R. R. *J. Mol. Biol.* **1976**, *100*, 399−413.
(35) Zipper, P.; Kriechbaum, M.; Durchschlag, H. *Prog. Colloid Polym. Sci.* **1993**, *93*, 376−377.
(36) Cölfen, H.; Völkel, A. *Eur. Biophys. J.* **2003**, *32*, 432−436.
(37) Kim, M.; Rho, Y.; Jin, K. S.; Ahn, B.; Jung, S.; Kim, H.; Ree, M. *Biomacromolecules* **2011**, *12*, 1629−1640.
(38) Kaltashov, I. A.; Mohimen, A. *Anal. Chem.* **2005**, *77*, 5370−5379.
(39) De Val, N.; Herschbach, H.; Potier, N.; Van Dorsselaer, A.; Crichton, R. R. *FEBS Lett.* **2006**, *580*, 6275−6280.
(40) Hoppler, M.; Zeder, C.; Walczyk, T. *Anal. Chem.* **2009**, *81*, 7368−7372.
(41) Zhu, B.; Ke, C.-H.; Huang, H.-Q. *Rapid Commun. Mass Spectrom.* **2011**, *25*, 2418−2424.
(42) Zeng, Q.; Reuther, R.; Oxsher, J.; Wang, Q. *Bioorg. Chem.* **2008**, *36*, 255−260.
(43) Lin, H.; Xu, C.; Qing, L.; Bin-Lin, Z.; He-Qing, H. *Chin. J. Anal. Chem.* **2007**, *35*, 1745−1750.
(44) Twerenbold, D.; Vuilleumier, J.; Gerber, D.; Tadsen, A.; van den Brandt, B.; Gillevet, P. M. *Appl. Phys. Lett.* **1996**, *68*, 3503−3505.
(45) Frank, M.; Labov, S. E.; Westmacott, G.; Benner, W. H. *Mass Spectrom. Rev.* **1999**, *18*, 155−186.
(46) Shiki, S.; Ukibe, M.; Sato, Y. *J. Mass Spectrom.* **2008**, *43*, 1686−1691.
(47) Banner, W. H.; Horn, D. M.; Jaklevic, J. M.; Frank, M.; Mears, C.; Labov, S.; Barfknecht, A. T. *J. Am. Soc. Mass Spectrom.* **1997**, *8*, 1094−1102.
(48) Wenzel, R. J.; Matter, U.; Schultheis, L.; Zenobi, R. *Anal. Chem.* **2005**, *77*, 4329−4337.
(49) Aksenov, A. A.; Bier, M. E. *J. Am. Soc. Mass Spectrom.* **2008**, *19*, 219−230.
(50) Ozdemir, A.; Aksenov, A. A.; Firek, B. A.; Hendrix, R. W.; Bier, M. E. In *Proceeding of the 55th ASMS Conference on Mass Spectrometry and Allied Topics*, Indianapolis, IN, June 3−7, 2007.
(51) Sipe, D. M.; Ozdemir, A.; Firek, B. A.; Hendrix, R. W.; Bier, M. E. In *Proceeding of the 56th ASMS Conference on Mass Spectrometry and Allied Topics*, Denver, CO, June 1−5, 2008.
(52) Banyard, S. H.; Stammers, D. K.; Harrison, P. M. *Nature* **1978**, *271*, 282−284.
(53) Clegg, G. A.; Stansfield; Robert, F. D.; Bourne, P. E.; Harrison, P. M. *Nature* **1980**, *288*, 298−300.
(54) Stefanini, S.; Cavallo, S.; Wang, C.; Tataseo, P.; Vecchini, P.; Giartosio, A.; Chiancone, E. *Arch. Biochem. Biophys.* **1996**, *325*, 58−64.
(55) Cavallo, S.; Mei, G.; Stefanini, S. *Protein Sci.* **1998**, *7*, 427−432.
(56) Chasteen, N. D.; Theil, E. C. *J. Biol. Chem.* **1982**, *257*, 7672−7677.
(57) Gerl, M.; Jaenicke, R. *Eur. Biophys. J.* **1987**, *15*, 103−109.
(58) Listowsky, I.; Blauer, G.; Englard, S.; Betheil, J. J. *Biochemistry* **1972**, *11*, 2176−2182.
(59) Suran, A.; Tarver, H. *Arch. Biochem. Biophys.* **1965**, *111*, 399−406.
(60) De Haën, C. *Anal. Biochem.* **1987**, *166*, 235−245.
(61) Wong, K. K. W.; Douglas, T.; Gider, S.; Awschalom, D. D.; Mann, S. *Chem. Mater.* **1998**, *10*, 279−285.
(62) Heusterspreute, M.; Crichton, R. *FEBS Lett.* **1981**, *129*, 322−327.



DOI: 10.1021/acs.analchem.5b02180
*Anal. Chem.* 2015, 87, 8985−8993

(63) Orino, K.; Miura, T.; Muto, S.; Watanabe, K. *DNA Sequence* **2005**, *16*, 58−64.
(64) Wong, K. K. W.; Colfen, H.; Whilton, N. T.; Douglas, T.; Mann, S. *J. Inorg. Biochem.* **1999**, *76*, 187−195.
(65) Fischbach, F. A.; Harrison, P. M.; Hoy, T. G. *J. Mol. Biol.* **1969**, *39*, 235−238.
(66) McKenzie, R. a; Yablonski, M. J.; Gillespie, G. Y.; Theil, E. C. *Arch. Biochem. Biophys.* **1989**, *272*, 88−96.



DOI: 10.1021/acs.analchem.5b02180
*Anal. Chem.* 2015, 87, 8985−8993